Published in final edited form as:
J Mol Med (Berl). 2014 February ; 92(2): 151–164. doi:10.1007/s00109-013-1102-5.

Ganetespib blocks HIF-1 activity and inhibits tumor growth, vascularization, stem cell maintenance, invasion, and metastasis in orthotopic mouse models of triple-negative breast cancer

Lisha Xiang[a,b,e], **Daniele M. Gilkes**[a,b], **Pallavi Chaturvedi**[a,b], **Weibo Luo**[a,c], **Hongxia Hu**[a,b], **Naoharu Takano**[a,b], **Houjie Liang**[e], and **Gregg L. Semenza**[a,b,c,d,*]

[a]Vascular Program, Institute for Cell Engineering Johns Hopkins University School of Medicine, Baltimore, MD 21205, USA

[b]McKusick-Nathans Institute of Genetic Medicine Johns Hopkins University School of Medicine, Baltimore, MD 21205, USA

[c]Department of Biological Chemistry Johns Hopkins University School of Medicine, Baltimore, MD 21205, USA

[d]Departments of Pediatrics, Oncology, Medicine, and Radiation Oncology Johns Hopkins University School of Medicine, Baltimore, MD 21205, USA

[e]Department of Oncology and Southwest Cancer Center Southwest Hospital, Third Military Medical University 30 Gaotanyan Street, Chongqing 400038, China

Abstract

Targeted therapy against triple-negative breast cancers, which lack expression of the estrogen, progesterone, and HER2 receptors, is not available and the overall response to cytotoxic chemotherapy is poor. One of the molecular hallmarks of triple-negative breast cancers is increased expression of genes that are transcriptionally activated by hypoxia-inducible factors (HIFs), which are implicated in many critical aspects of cancer progression including metabolism, angiogenesis, invasion, metastasis, and stem cell maintenance. Ganetespib is a second-generation inhibitor of heat shock protein 90 (HSP90), a molecular chaperone that is essential for the stability and function of multiple client proteins in cancer cells including HIF-1α. In this study, human MDA-MB-231 and MDA-MB-435 triple-negative breast cancer cells were injected into the mammary fat pad of immunodeficient mice that received weekly intravenous injections of ganetespib or vehicle following the development of palpable tumors. Ganetespib treatment markedly impaired primary tumor growth and vascularization, and eliminated local tissue invasion and distant metastasis to regional lymph nodes and lungs. Ganetespib treatment also significantly reduced the number of Aldefluor-positive cancer stem cells in the primary tumor. Primary tumors of ganetespib-treated mice had significantly reduced levels of HIF-1α (but not HIF-2α) protein and of HIF-1 target gene mRNAs encoding proteins that play key roles in angiogenesis, metabolism, invasion, and metastasis, thereby providing a molecular basis for observed effects of the drug on the growth and metastasis of triple-negative breast cancer.

*Correspondence: gsemenza@jhmi.edu; Fax: 443-287-5618.

Disclosure statement All authors confirm that there is no conflict of interest associated with this publication.

Keywords

Hypoxia-inducible factor 1; Ganetespib; Hsp90 inhibitor; Breast cancer metastasis; Cancer stem cell

Introduction

Metastasis is the final step in the progression of solid malignancies and the major cause of mortality in breast cancer patients. Intratumoral hypoxia is a characteristic property of advanced breast cancers that is associated with a significantly increased risk of metastasis [1]. Hypoxia-inducible factors (HIFs) activate the transcription of target genes that are involved in many aspects of breast cancer progression, such as angiogenesis, lymphangiogenesis, metabolic reprogramming, local tissue invasion, and metastasis by activating specific batteries of target genes [2, 3]. First, HIFs activate the transcription of genes encoding angiogenic growth factors, including vascular endothelial growth factor (VEGF) and stromal-derived factor 1 (SDF1), which play important roles in tumor vascularization [4, 5]. Second, HIFs regulate genes encoding proteins that mediate the switch from oxidative to glycolytic metabolism, including glucose transporter 1 (GLUT1), hexokinase 1 (HK1), HK2, and pyruvate dehydrogenase kinase 1 (PDK1) [3]. Third, HIFs activate transcription of genes encoding proteins, such as the collagen prolyl-4-hydroxylases (P4HA1 and P4HA2) and matrix metalloproteinase 9 (MMP9), which play key roles in local tissue invasion through remodeling of the extracellular matrix [6–8]. Fourth, HIFs control expression of genes encoding proteins, such as angiopoietin-like 4 (ANGPTL4), L1 cell adhesion molecule (L1CAM), and lysyl oxidase (LOX) that are required for metastasis [9–11]. Finally, HIF-1 has been implicated in the maintenance of tumor-initiating cells or cancer stem cells, although specific HIF target genes involved in this process have not been identified [12, 13].

HIFs are heterodimeric transcription factors composed of an O_2-regulated HIF-1α or HIF-2α subunit and a constitutively expressed HIF-1β subunit [14, 15]. Under normoxic conditions, proline hydroxylase domain protein 2 (PHD2) catalyzes hydroxylation of HIF-1α and HIF-2α, which is required for binding of the von Hippel-Lindau (VHL) tumor suppressor protein and the VHL-dependent recruitment of an Elongin C-containing ubiquitin ligase that targets HIF-1α and HIF-2α for ubiquitination and degradation by the 26*S* proteasome [15]. Also under normoxic conditions, asparagine hydroxylation by factor inhibiting HIF-1 (FIH-1) blocks binding of coactivators to the transactivation domain of HIF-1α and HIF-2α [15]. Under hypoxic conditions, PHD2 and FIH-1 activity are inhibited, leading to HIF-1α and HIF-2α protein stabilization, dimerization with HIF-1β, DNA binding, coactivator recruitment, and target gene transactivation. Heat shock protein 90 (HSP90) is a molecular chaperone that binds to HIF-1α and is required for its stability prior to dimerization with HIF-1β [16–19]. Studies of the first-generation HSP90 inhibitors geldanamycin and 17-allylaminogeldanamycin revealed that displacement of HSP90 from HIF-1α allowed binding of the scaffold protein RACK1, which recruited Elongin C, leading to the ubiquitination and proteasomal degradation of HIF-1α [20], regardless of the O_2 concentration or VHL status of the cell [17].

Targeted therapies are available for breast cancers that express the estrogen/progesterone receptors (ER/PR), which are treated with tamoxifen or aromatase inhibitors, and those that express HER2, which are treated with trastuzumab or tyrosine kinase inhibitors. In contrast, targeted therapy is not available for triple-negative breast cancers that lack expression of the estrogen, progesterone, and HER2 receptors, account for ~15% of breast cancer cases, are treated with cytotoxic chemotherapy, and are associated with increased mortality compared

to other breast cancer subtypes [21]. Several second-generation HSP90 inhibitors have been shown to inhibit the proliferation and survival of ER^+/PR^+, $HER2^+$, and triple-negative breast cancer cell lines in vitro and in subcutaneous tumor xenografts, which is associated with degradation of multiple HSP90 client proteins [22–24].

Ganetespib (STA-9090) is a triazolone compound that is structurally unrelated to first-generation HSP90 inhibitors, with a superior antitumor activity and safety profile [25]. The x-ray crystal structure of ganetespib bound to the ATP pocket at the amino-terminus of HSP90 has been reported, providing a molecular basis for its inhibitory effect [25]. Ganetespib binding disrupts the interaction of HSP90 with the co-chaperone p23, which is required for efficient chaperone function [26]. In this study, we demonstrate for the first time that in addition to inhibiting primary tumor growth and vascularization, ganetespib blocks lymphatic and vascular metastasis of triple-negative breast cancer cells and impairs cancer stem cell maintenance in an orthotopic mouse model. We provide molecular evidence that decreased expression of HIF-1α and HIF-1 target genes plays an important role in the therapeutic effects of ganetespib.

Materials and methods

Cell culture

Human MDA-MB-231 and MDA-MB-435 breast cancer cells were obtained from the NCI PS-OC Network Bioresource Core Facility (National Institutes of Health) and cultured in Dulbecco's modified essential medium supplemented with 10% fetal bovine serum and 1% penicillin–streptomycin (Invitrogen) in a 5% CO_2/95% air incubator at 37°C. The MDA-MB-231 and MDA-MB-435 cell lines were each authenticated by short tandem repeat profiling and tested negative for the presence of mycoplasma using a PCR-based assay. Cultured cells were pretreated with 100 nM ganetespib or vehicle for 30 min, exposed to 20% or 1% O_2 for 6 h in the continued presence of drug, and then lysed for immunoblot assays.

Drug preparation

Ganetespib [3-(2,4-dihydroxy-5-isopropylphenyl)-4-(1-methyl-1H-1,2,4-triazol-5(4H)-one] was synthesized by Synta Pharmaceuticals Corp. and prepared as a stock solution in DMSO. For administration, ganetespib was formulated in vehicle consisting of 10% DMSO, 18% Cremophor RH 40, 3.6% dextrose, and 68.4% water [24].

Orthotopic implantation

Studies using 6-to-8 week-old female severe combined immunodeficiency (SCID) mice (NCI) were performed according to protocols approved by the Johns Hopkins University Animal Care and Use Committee in accordance with the NIH Guide for the Care and Use of Laboratory Animals. Cells were harvested from tissue culture plates by trypsinization, resuspended at 10^7 cells/ml in a 50:50 mixture of PBS:Matrigel (BD Biosciences), and 2×10^6 cells were injected into the mammary fat pad. Tumor length (L), width (W) and thickness (T) were measured (in mm) using calipers and tumor volume (V) was calculated as $V = 0.52\times L\times W\times T$. After palpable tumors formed (7 days after tumor implantation), mice received a tail vein injection of ganetespib (150 mg/kg) or vehicle, which was repeated every 7 days. Tumor volume and body weight were monitored twice per week. Mice were euthanized 44 days after tumor implantation and 24 hours after the last drug treatment. Following euthanasia, the left lung was inflated with low-melting-point agarose for formalin fixation, paraffin embedding, staining of tissue sections with hematoxylin and eosin (H&E), and immunohistochemistry. Portions of the right lung were used for the isolation of genomic DNA. Primary tumors were harvested for isolation of total RNA and protein lysate

preparation. Blood was collected by heart puncture for RNA isolation. The axillary lymph node ipsilateral to the primary tumor was processed for immunohistochemistry [27].

Extraction of genomic DNA

Lung tissue was digested with proteinase K at 55°C overnight, and genomic DNA was extracted with phenol and chloroform, and precipitated with isopropanol. 200 ng of genomic DNA was used for quantitative real-time PCR (qPCR) using the following human *HK2* gene-specific primers to quantify lung metastatic burden: ccagttcattcacatcatcag and cttacacgaggtcacatagc. The result was normalized to the result obtained using primers that bind to both human and mouse 18S rRNA genes: cggcgacgacccattcgaac and gaatcgaaccctgattccccgtc.

Reverse transcription-qPCR (RT-qPCR)

Total RNA was extracted from using TRIzol (Invitrogen) and treated with DNase I (Ambion). 1 μg of total RNA was used for first-strand cDNA synthesis using iScript cDNA Synthesis system (BioRad), and qPCR was performed using human-specific primers and SYBR Green qPCR Master Mix (Fermentas). For each primer pair, the annealing temperature was optimized by gradient PCR. The expression (E) of each target mRNA relative to human 18S rRNA in tumors from ganetespib- vs vehicle-treated mice was calculated based on the cycle threshold (Ct) as $E = 2^{-\Delta(\Delta Ct)}$, in which $\Delta Ct = Ct_{target} - Ct_{18S}$ and $\Delta(\Delta Ct) = \Delta Ct_{ganetespib} - \Delta Ct_{vehicle}$ 28]. The nucleotide sequence of the primers is as follows: 18S rRNA, gaggatgaggtggaacgtgt and agaagtgacgcagccctcta; ALDH1A1, ctgctggcgacaatggagt and cgcaatgttttgatgcagcct; ALDH1A3, tgaatggcacgaatccaagag and cacgtcgggcttatctcct; ANGPTL4, tccaccgacctcccgttag and ctgttctgagccttgagttgtg; GLUT1, cgggccaagagtgtgctaaa and tgacgataccggagccaatg; HK2, ccagttcattcacatcatcag and cttacacgaggtcacatagc; L1CAM, gccacctgtcatcacggaac and gtccagcggaactgcacttc; LOX, gttccaagctggctactc and gggttgtcgtcagagtac; MMP9, gggacgcagacatcgtcatc and tcgtcatcgtcgaaatgggc; P4HA1, ccctgagactggaaaattgaccacagc and ggggttcatactgtcctccaactcca; P4HA2, gcctgcgctggaggaccttg and tgtgcctgggtccagcctgt; PDK1, ggattgcccatatcacgtcttt and tcccgtaaccctctagggaata; RPL13A, gaggcgagggtgatagag and acacacaagggtccaattc; SDF-1, actttagcttcgggtcaatgc and actttagcttcgggtcaatgc; and VEGF, cttgccttgctgctctac and tggcttgaagatgtactcg.

Immunoblot assays

Whole cell lysates were prepared in RIPA lysis buffer. Blots were probed with HIF-1α (1:1000, BD Transduction Laboratory), HIF-2α (1:500, Novus Biologicals) and HIF-1β (1:2000, Novus Biologicals) antibodies. HRP-conjugated anti-rabbit (Roche) and anti-mouse (Santa Cruz) secondary antibodies were used. Chemiluminescent signal was developed using ECL Plus (GE Healthcare).

Tumor hypoxia assay

Pimonidazole (Hypoxyprobe-1) was administered by intraperitoneal injection (60 mg/kg), and 60 min later the primary tumor was harvested, placed in 10% formalin, and processed for immunohistochemistry using an anti-pimonidazole antibody (Natural Pharmacia International).

Immunohistochemistry

Primary tumors and ipsilateral axillary lymph nodes were fixed in 10% formalin and paraffin embedded. Sections were dewaxed by xylene, hydrated with graded ethanols, followed by antigen retrieval using citrate buffer (pH 6.1). The LSAB+ System HRP kit (DAKO) was used with antibodies against vimentin (1:200, Santa Cruz), CD31 (1:20,

Dianova, Germany), P4HA1 (1:100, Novus Biologicals), pimonidazole (1:100, Natural Pharmacia International), and Ki67 (1:100, Novus Biologicals). Sections werre counterstained with Mayer's hematoxylin (Sigma). HIF-1α immunohistochemistry was performed as described [29].

Digital image analysis

Immunohistochemical staining was quantified by Image J software (NIH). The acquired images in RGB color were separated into different color channels by a deconvolution method [30]. The Image J plug-in for color deconvolution has a built-in vector for separating hematoxylin and diaminobenzidine (DAB) staining. After color deconvolution, hematoxylin and DAB images were processed separately. By using 6-8 random fields per tumor section stained with the antibody of interest, suitable threshold levels for hematoxylin and DAB were determined. These thresholds were used on both hematoxylin and DAB images and kept constant for analysis of the main image dataset. The extent of staining was calculated as the DAB-positive area divided by the hematoxylin-positive area. Six to eight ×40 fields, which encompassed the total surface area of each histological section, were analyzed. HIF-1α and Ki67 staining were calculated as the number of DAB-stained cells divided by the number of total cells per field. Vimentin, P4HA1 and pimonidazole staining were calculated as the DAB-positive area divided by the total tissue area per field. Blood vessel area was calculated as CD31-positive pixels divided by the total tissue area per field.

Aldefluor assay

To prepare primary tumor cells for flow cytometry analysis, tumor tissue was minced and digested with 1 mg/mL of type 1 collagenase (Sigma) at 37 °C for 30 min. Digested tissue was filtered through a 70-μm cell strainer. The Aldefluor kit (Stem Cell Technologies) was used for fluorometric determination of aldehyde dehydrogenase activity. 1×10^6 cells obtained from freshly dissociated tumors were suspended in assay buffer containing the fluorescent substrate BODIPY aminoacetaldehyde (1 μmol/L) and incubated for 40 min at 37°C. As a negative control, for each tumor sample, an aliquot of cells was treated with the aldehyde dehydrogenase inhibitor diethylaminobenzaldehyde (DEAB; 50 mmol/L). Samples were subjected to flow cytometry analysis (FACScalibur, BD Biosciences).

Statistical Analysis

All data were expressed as mean ± SEM. When data were not Gaussian, a logarithmic or square root transformation was applied. Differences between experimental groups were assessed using Student's test or two-way ANOVA. A p value of < 0.05 was considered statistically significant.

Results

Ganetespib treatment selectively inhibits accumulation of HIF-1α in hypoxic breast cancer cells

To investigate the effect of ganetespib on the accumulation of HIF-1α and HIF-2β in response to hypoxia, MDA-MB-231 [31] and MDA-MB-435 [32] triple-negative breast cancer cells were pre-treated with 100 nM ganetespib or vehicle for 30 min and then exposed to 20% or 1% O_2 in the continued presence of drug for 6 h. Immunoblot assays revealed that hypoxia-induced accumulation of HIF-1α was markedly reduced, whereas HIF-2β levels were only modestly reduced (MDA-MB-231) or unaffected (MDA-MB-231) by ganetespib treatment (Figure 1). Thus, ganetespib selectively inhibits accumulation of HIF-1α in human triple-negative breast cancer cells.

Ganetespib treatment inhibits primary tumor growth and vascularization after orthotopic implantation of MDA-MB-231 cells

MDA-MB-231 human triple-negative breast cancer cells were implanted in the mammary fat pad of SCID mice. When tumors became palpable on day 7 after implantation, mice were randomized to treatment with ganetespib (150 mg/kg) or vehicle (N = 9 mice in each group) by tail vein injection every 7 days over a six-week period. The growth of primary tumors in mice treated with ganetespib was significantly decreased compared with tumors in mice treated with vehicle (Fig. 2a). There was no significant difference in body weight in ganetespib or vehicle treated mice between the start point and end point of the study on day 44 (Fig. 2b). The final weight of tumors from ganetespib treated mice was significantly decreased compared to tumors from vehicle treated mice (Fig. 2c). Consistent with the reduction in tumor growth, Ki67 staining (Fig. 2d) was significantly decreased in tumors from ganetespib treated mice (Fig. 2g). CD31 immunohistochemistry (Fig. 2e) revealed that blood vessel density was significantly decreased in tumors from ganetespib treated mice (Fig. 2h), which was associated with increased intratumoral hypoxia (Fig. 2i) as demonstrated by pimonidazole staining (Fig. 2f). Thus, ganetespib treatment significantly reduced the growth and vascularization of primary tumors following orthotopic transplantation of human breast cancer cells. These results are consistent with those previously observed in mice bearing subcutaneous xenografts of non-small cell lung cancer cells [26].

Ganetespib treatment inhibits HIF-1α expression, invasion, and metastasis

Immunohistochemical analysis of HIF-1α expression revealed strong nuclear staining at the tumor margin (Fig. 3a-b) and in central perinecrotic regions (Fig. 3c-d) of tumor sections from vehicle treated mice but not from ganetespib treated mice. In addition to the lack of HIF-1α expression, the invasion of cancer cells into the surrounding stroma that was characteristic of the tumor margin in vehicle treated mice was completely lost in ganetespib treated mice, which showed a well-demarcated tumor-stroma border in all cases (Fig. 3a). We previously demonstrated that HIF-1-dependent expression of P4HA1 was required for invasion and that MDA-MB-231 subclones in which P4HA1 expression was inhibited showed a strikingly similar loss of the invasive front [8]. Immunohistochemical detection of P4HA1 revealed a significant loss of expression in ganetespib treated mice (Fig. 3e-f).

To quantify the effect of ganetespib treatment on the expression of HIF subunits and HIF target gene products, we prepared tissue lysates and isolated total RNA from primary tumors. Immunoblot assays revealed a dramatic decrease in HIF-1α protein levels in the primary tumors of ganetespib treated mice, whereas levels of HIF-2α and HIF-1β were not affected by drug treatment (Fig. 4a-b). RT-qPCR analyses (Fig. 4c) revealed a significant decrease in the levels of HIF-regulated mRNAs encoding proteins involved in glucose metabolism (GLUT1, HK2, PDK1), angiogenesis (VEGF), invasion (P4HA1), and metastasis (ANGPTL4, L1CAM, LOX). In contrast, expression of RPL13A mRNA, which is not regulated by HIF-1, was unaffected by drug treatment.

The spontaneous metastasis of breast cancer cells from the primary tumor was examined by H&E staining of lung sections (Fig. 5a) to quantify the number of metastatic foci (Fig. 5b) and by a sensitive qPCR assay of lung genomic DNA using primers that were specific for the human *HK2* gene to determine the total lung metastatic burden (Fig. 5c). Remarkably, despite widespread metastases in vehicle treated mice, no metastatic foci were observed and human *HK2* DNA was not detected in lungs from ganetespib treated mice. As a final measure of metastasis via blood vessels, we collected peripheral blood and screened for the presence of circulating tumor cells (CTCs) using a sensitive RT-qPCR assay that was

specific for human 18S rRNA. CTCs were present in blood from vehicle treated mice but absent in blood from ganetespib treated mice (Fig. 5d).

Lymphatic dissemination to the ipsilateral axillary lymph node was analyzed by immunohistochemistry with an antibody specific for human vimentin. Lymph nodes from vehicle treated mice were markedly increased in size and displayed extensive staining for human vimentin, whereas no vimentin staining was observed in lymph nodes from ganetespib treated mice (Fig. 5e, f). Thus, ganetespib treatment completely eliminated metastasis of MDA-MB-231 breast cancer cells via blood vessels to the lungs and via lymphatics to the axillary lymph nodes.

Ganetespib inhibits primary tumor growth, vascular invasion, metastasis, and HIF target gene expression after orthotopic implantation of MDA-MB-435 cells

To confirm the results obtained after ganetespib treatment of mice orthotopically implanted with MDA-MB-231 cells, another human triple-negative breast cancer cell line, MDA-MD-435 (provenance of these cells is discussed in ref. 32), was used for mammary fat pad injection. Once again, ganetespib dramatically inhibited primary tumor growth over 6 weeks (Fig. 6a), with no effect on body weight (Fig. 6b), leading to a marked reduction in final tumor weight (Fig. 6c). Ganetespib treatment also abrogated the metastasis of MDA-MD-435 cells from the breast to the lungs, as determined by histology (Fig. 6d, e) and by qPCR (Figure 6f), and eliminated CTCs (Fig. 6g). Analysis of total RNA isolated from primary tumors demonstrated a significant reduction in the expression of a panel of HIF target genes required for angiogenesis (SDF-1, VEGF), invasion (P4HA2, MMP9), and metastasis (ANGPTL4) but no change in the expression of RPL13A mRNA (Fig. 6h).

Ganetespib treatment decreases the Aldefluor$^+$ cancer stem cell population in primary tumors

A distinct subpopulation of cells within a breast tumor, designated cancer stem cells or tumor initiating cells, is uniquely endowed with the capacity to regenerate a tumor and to form metastases, and these cancer stem cells can be identified by their expression of aldehyde dehydrogenase activity as measured by the Aldefluor assay [12, 33]. Following mammary fat pad implantation of MDA-MB-231 cells, the percentage of Aldefluor$^+$ cells decreased from 3.5% in tumors from vehicle treated mice to 1% in tumors from ganetespib treated mice, a reduction of >70% (Fig. 7a, b). Levels of ALDH1A1 and ALDH1A3 mRNA, which encode the aldehyde dehydrogenases whose activity is measured by the Aldefluor assay [34, 35], were significantly decreased in tumors from ganetespib treated mice (Fig. 7c). For MDAMB-435 cells, Aldefluor$^+$ cells decreased from 2.5% in primary tumors from vehicle treated mice to < 1% in tumors from ganetespib treated mice (Fig. 7d, e). Again, ALDH1A1 and ALDH1A3 mRNA levels were significantly decreased in tumors from ganetespib treated mice (Fig. 7f). To determine whether ALDH expression was directly HIF-regulated, cultured cells were exposed to 20% or 1% O_2 for 24 h. Neither ALDH1A1 nor ALDH1A3 mRNA expression was significantly induced by exposure of MDA-MB-231 (Fig. 7g) or MDA-MB-435 (Fig. 7h) cells to hypoxia.

Discussion

Previous studies have demonstrated that HSP90 inhibitors block the growth of established tumor xenografts after subcutaneous injection of human breast cancer cells into immunodeficient mice [22–24]. In this study, we demonstrate for the first time that the second-generation HSP90 inhibitor ganetespib blocks the metastasis of human breast cancer cells when administered to mice intravenously on a once weekly schedule. Treatment was initiated after the primary tumor became palpable, 1 week after implantation of breast cancer

cells into the mammary fat pad, when metastatic niche formation has already been initiated. Specifically, in the case of metastatic niche formation in the lungs of mice bearing MDA-MB-435 orthotopic tumors, collagen fiber formation in the lungs occurs within 8 days, bone marrow-derived cell recruitment to the lungs occurs within 16 days, and cancer cells are found with the metastatic niche within 24 days after implantation of cancer cells in the mammary fat pad [10]. Despite the rapid kinetics of metastasis in this model, weekly administration of ganetespib starting on day 7 was sufficient to completely eliminate lung metastasis.

Although HSP90 inhibitors have been shown previously to induce the degradation of many kinases (AKT, C-RAF, EGFR, ERK, GSK3, IGF-1Rβ, JNK, mTOR, SRC), transcription factors (C-JUN, MYC, STAT3, NF-κB p65, YAP) and other HSP90 client proteins that may contribute to breast cancer progression [22–24], we demonstrate that treatment of tumor-bearing mice with ganetespib resulted in decreased HIF-1α levels within the tumor, which was associated with decreased expression of multiple mRNA products of known HIF-1 target genes that have been shown to play essential roles in breast cancer angiogenesis, metabolism, invasion, and metastasis (Fig. 8). Ganetespib treatment inhibited the expression of SDF1 and VEGF mRNA, which was associated with decreased tumor vascularization. Decreased expression of multiple angiogenic factors was observed in colon cancer biopsies from patients treated with ganetespib [36]. Ganetespib treatment completely eliminated lung metastases and circulating tumor cells, which was associated with decreased expression of ANGPTL4, LOX, P4HA1, and P4HA2. Previous studies have demonstrated that HIF-1 directly activates transcription of the *ANGPTL4*, *LOX*, *P4HA1*, and *P4HA2* genes in MDA-MB-231 cells and that knockdown of expression of any one of these genes eliminates lung metastasis [8, 9, 11]. Taken together, these results suggest that inhibition of HIF-1α expression contributed to the anti-metastatic effect of ganetespib treatment.

In contrast to HIF-1α, HIF-2α protein levels were not reduced in the tumors of ganetespib treated mice or in breast cancer cells cultured under hypoxic conditions. HIF-2α was reported to interact with HSP90 [19], but overexpression of RACK1 in HEK293T cells only modestly decreased HIF-2α levels, whereas HIF-1α was efficiently degraded [20], suggesting that HIF-1α may be more dependent upon HSP90 for stability. We have previously demonstrated that expression of short hairpin RNA targeting HIF-1α in MDA-MB-231 or MDA-MB-435 cells is sufficient to inhibit primary tumor growth and metastasis [10, 11]. Further studies are warranted to determine whether the preferential sensitivity of HIF-1α to ganetespib treatment is observed in other contexts.

We also show for the first time that ganetespib treatment reduced the Aldefluor$^+$ breast cancer stem cell population in vivo, which was associated with decreased expression of mRNAs encoding the aldehyde dehydrogenase isoforms ALDH1A1 and ALDH1A3. However, ALDH1A1 and ALDH1A3 mRNA expression was not induced when MDA-MB-231 and MDA-MB-435 cells were exposed to hypoxia for 24 h, indicating that HIF-1 does not directly regulate the expression of these genes. Thus, aldehyde dehydrogenase activity is a biomarker for the cancer stem cell phenotype and the target genes regulated by HIF-1 that directly contribute to this phenotype remain to be identified. Inhibitory effects on other HSP90 client proteins may also contribute to the reduction in Aldefluor$^+$ cells in the primary tumors of ganetespib-treated mice. However, our results are consistent with previous reports demonstrating that exposure of cultured MDA-MB-231 and SUM159 triple-negative breast cancer cells to hypoxia for 2 to 6 days increased the Aldefluor$^+$ population by 2- to 4-fold in a HIF-1α-dependent and HIF-2α-independent manner [12]. The decreased Aldefluor$^+$ population in ganetespib-treated tumors stands in contrast to the increased Aldefluor$^+$ population that was observed in response to paclitaxel treatment of

tumors derived from injection of MDA-MB-231 and other triple-negative breast cancer cell lines [37].

Thus, inhibition of HIF-1 regulated genes provides a molecular basis for the effects of ganetespib treatment on angiogenesis (SDF-1, VEGF), local tissue invasion and intravasation as measured by CTCs (P4HA1, P4HA2, MMP9), and lung metastasis, which requires CTCs to marginate (L1CAM) and extravasate (ANGPTL4) at sites of metastatic niche formation (LOX) and then, if they possess stem cell properties, to form a secondary tumor. The observed alterations in gene expression provide molecular evidence that inhibition of the HIF-regulated transcriptional program by ganetespib treatment contributed to the dramatic abrogation of lymphatic and vascular metastasis that was observed following orthotopic transplantation of two independent triple-negative breast cancer cell lines.

Our preclinical study was focused on triple-negative breast cancer because of the poor clinical outcome that is associated with cytotoxic chemotherapy, such as paclitaxel, which remains the standard of care in the absence of any available targeted therapy [21]. HIF-1 target gene expression represents a signature of basal/triple-negative breast cancers [38] and the results of the present study suggest that ganetespib may have therapeutic benefit in this patient population, either alone or in combination with cytotoxic chemotherapy. A phase II clinical trial (Clinicaltrials.gov identifier: NCT01677455) is currently underway to evaluate the effectiveness of intravenous administration of ganetespib (150 mg/m^2 twice weekly) to women with triple-negative (or HER2$^+$) breast cancer. HIF-1α overexpression is associated with a significantly increased risk of metastasis and mortality in many other cancer types [39] and further studies are required to investigate whether ganetespib treatment may be beneficial in other clinical contexts in which targeted therapies are not available.

Acknowledgments

We thank Karen Padgett (Novus Biologicals) for providing antibodies against HIF-1β, HIF-2α, Ki67, and P4HA1. This work was supported in part by a sponsored research agreement with Synta Pharmaceuticals Corp., which provided ganetespib and vehicle but had no involvement in the experimental design, data analysis, or manuscript preparation.

G.L.S. is the C. Michael Armstrong Professor at the Johns Hopkins University School of Medicine and an American Cancer Society Research Professor. L.X., D.M.G., and W.L. were supported by grants from the Chinese Scholarship Council, Susan G. Komen Foundation, and National Cancer Institute (K99-CA168746), respectively.

References

1. Vaupel P, Hockel M, Mayer A. Detection and characterization of tumor hypoxia using pO_2 histography. Antioxid Redox Signal. 2007; 9:1221–1235. [PubMed: 17536958]
2. Semenza GL. Cancer-stromal cell interactions mediated by hypoxia-inducible factors promote angiogenesis, lymphangiogenesis, and metastasis. Oncogene. 2013; 32:4057–4063. [PubMed: 23222717]
3. Semenza GL. HIF-1 mediates metabolic responses to intratumoral hypoxia and oncogenic mutations. J Clin Invest. 2013; 123:3664–3671. [PubMed: 23999440]
4. Forsythe JA, Jiang BH, Iyer NV, Agani F, Leung SW, Koos RD, Semenza GL. Activation of vascular endothelial growth factor gene transcription by hypoxia-inducible factor 1. Mol Cell Biol. 1996; 16:4604–4613. [PubMed: 8756616]
5. Ceradini DJ, Kulkarni AR, Callaghan MJ, Tepper OM, Bastidas N, Kleinman ME, Capla JM, Galiano RD, Levine JP, Gurtner GC. Progenitor cell trafficking is regulated by hypoxic gradients through HIF-1 induction of SDF-1. Nat Med. 2004; 10:858–864. [PubMed: 15235597]
6. Chaturvedi P, Gilkes DM, Wong CC, Kshitiz, Luo W, Zhang H, Wei H, Takano N, Schito L, Levchenko A, et al. Hypoxia-inducible factor-dependent breast cancer-mesenchymal stem cell

bidirectional signaling promotes metastasis. J Clin Invest. 2013; 123:189–205. [PubMed: 23318994]

7. Choi JY, Jang YS, Min SY, Song JY. Overexpression of MMP-9 and HIF-1α in breast cancer cells under hypoxic conditions. J Breast Cancer. 2011; 14:88–95. [PubMed: 21847402]
8. Gilkes DM, Chaturvedi P, Bajpai S, Wong CC, Wei H, Pitcairn S, Hubbi ME, Wirtz D, Semenza GL. Collagen prolyl hydroxylases are essential for breast cancer metastasis. Cancer Res. 2013; 73:3285–3296. [PubMed: 23539444]
9. Erler JT, Bennewith KL, Nicolau M, Dornhöfer N, Kong C, Le QT, Chi JT, Jeffrey SS, Giaccia AJ. Lysyl oxidase is essential for hypoxia-induced metastasis. Nature. 2006; 440:1222–1226. [PubMed: 16642001]
10. Wong CC, Gilkes DM, Zhang H, Chen J, Wei H, Chaturvedi P, Fraley SI, Wong CM, Khoo US, Ng IO, et al. Hypoxia-inducible factor 1 is a master regulator of breast cancer metastatic niche formation. Proc Natl Acad Sci U S A. 2011; 108:16369–16374. [PubMed: 21911388]
11. Zhang H, Wong CC, Wei H, Gilkes DM, Korangath P, Chaturvedi P, Schito L, Chen J, Krishnamachary B, Winnard PT Jr, et al. HIF-1-dependent expression of angiopoietin-like 4 and L1CAM mediates vascular metastasis of hypoxic breast cancer cells to the lungs. Oncogene. 2012; 31:1757–1770. [PubMed: 21860410]
12. Conley SJ, Gheordunescu E, Kakarala P, Newman B, Korkaya H, Heath AN, Clouthier SG, Wicha MS. Antiangiogenic agents increase breast cancer stem cells via the generation of tumor hypoxia. Proc Natl Acad Sci U S A. 2012; 109:2784–2789. [PubMed: 22308314]
13. Schwab LP, Peacock DL, Majumdar D, Ingels JF, Jensen LC, Smith KD, Cushing RC, Seagroves TN. Hypoxia-inducible factor 1 promotes primary tumor growth and tumor-initiating cell activity in breast cancer. Breast Cancer Res. 2012; 14:R6. [PubMed: 22225988]
14. Wang GL, Jiang BH, Rue EA, Semenza GL. Hypoxia-inducible factor 1 is a basic-helix-loop-helix-PAS heterodimer regulated by cellular O_2 tension. Proc Natl Acad Sci U S A. 1995; 92:5510–5514. [PubMed: 7539918]
15. Prabhakar NR, Semenza GL. Adaptive and maladaptive cardiorespiratory responses to continuous and intermittent hypoxia mediated by hypoxia-inducible factors 1 and 2. Physiol Rev. 2012; 92:967–1003. [PubMed: 22811423]
16. Minet E, Mottet D, Michel G, Roland I, Raes M, Remacle J, Michiels C. Hypoxia-induced activation of HIF-1: role of HIF-1α-Hsp90 interaction. FEBS Lett. 1999; 460:251–256. [PubMed: 10544245]
17. Isaacs JS, Jung YJ, Mimnaugh EG, Martinez A, Cuttitta F, Neckers LM. Hsp90 regulates a von Hippel Lindau-independent hypoxia-inducible factor-1α-degradative pathway. J Biol Chem. 2002; 277:29936–29944. [PubMed: 12052835]
18. Isaacs JS, Jung YJ, Neckers L. Aryl hydrocarbon nuclear translocator (ARNT) promotes oxygen-independent stabilization of hypoxia-inducible factor-1α by modulating an Hsp90-dependent regulatory pathway. J Biol Chem. 2004; 279:16128–16135. [PubMed: 14764593]
19. Katschinski DM, Schindler SG, Thomas T, Voss AK, Wenger RH. Interaction of the PAS B domain with HSP90 accelerates hypoxia-inducible factor 1α stabilization. Cell Physiol Biochem. 2004; 14:351–360. [PubMed: 15319539]
20. Liu YV, Baek JH, Zhang H, Diez R, Cole RN, Semenza GL. RACK1 competes with HSP90 for binding to HIF-1α and is required for O_2-independent and HSP90 inhibitor-induced degradation of HIF-1α. Mol Cell. 2007; 25:207–217. [PubMed: 17244529]
21. Cleator S, Heller W, Coombes RC. Triple-negative breast cancer: therapeutic options. Lancet Oncol. 2007; 8:235–244. [PubMed: 17329194]
22. Caldas-Lopes E, Cerchietti L, Ahn JH, Clement CC, Robles AI, Rodina A, Moulick K, Taldone T, Gozman A, Guo Y, et al. Hsp90 inhibitor PU-H71, a multimodal inhibitor of malignancy, induces complete responses in triple-negative breast cancer models. Proc Natl Acad Sci U S A. 2009; 106:8368–8373. [PubMed: 19416831]
23. Mehta PP, Whalen P, Baxi SM, Kung PP, Yamazaki S, Yin M. Effective targeting of triple-negative breast cancer cells by PF-4942847, a novel oral inhibitor of Hsp90. Clin Cancer Res. 2011; 17:5432–5442. [PubMed: 21715568]

24. Friedland JC, Smith DL, Sang J, Acquaviva J, He S, Zhang C, Proia DA. Targeted inhibition of Hsp90 by ganetespib is effective across a broad spectrum of breast cancer subtypes. Invest New Drugs. 2013 2013 May 18 [Epub ahead of print].
25. Ying W, Du Z, Sun L, Foley KP, Proia DA, Blackman RK, Zhou D, Inoue T, Tatsuta N, Sang J, et al. Ganetespib, a unique triazolone-containing Hsp90 inhibitor, exhibits potent antitumor activity and a superior safety profile for cancer therapy. Mol Cancer Ther. 2012; 11:475–484. [PubMed: 22144665]
26. Shimamura T, Perera SA, Foley KP, Sang J, Rodig SJ, Inoue T, Chen L, Li D, Carretero J, Li Y, et al. Ganetespib (STA-9090), a nongeldanamycin HSP90 inhibitor, has potent antitumor activity in in vitro and in vivo models of non-small cell lung cancer. Clin Cancer Res. 2012; 18:4973–4985. [PubMed: 22806877]
27. Schito L, Rey S, Tafani M, Zhang H, Wong CC, Russo A, Russo MA, Semenza GL. Hypoxia-inducible factor 1-dependent expression of platelet-derived growth factor B promotes lymphatic metastasis of hypoxic breast cancer cells. Proc Natl Acad Sci U S A. 2012; 109:E2707–E2716. [PubMed: 23012449]
28. Lee K, Zhang H, Qian DZ, Rey S, Liu JO, Semenza GL. Acriflavine inhibits HIF-1 dimerization, tumor growth, and vascularization. Proc Natl Acad Sci U S A. 2009; 106:17910–17915. [PubMed: 19805192]
29. Krishnamachary B, Semenza GL. Analysis of hypoxia-inducible factor 1α expression and its effects on invasion and metastasis. Methods Enzymol. 2007; 435:347–354. [PubMed: 17998062]
30. Ruifrok AC, Johnston DA. Quantification of histochemical staining by color deconvolution. Anal Quant Cytol Histol. 2001; 23:291–299. [PubMed: 11531144]
31. Cailleau R, Young R, Olive M, Reeves WJ Jr. Breast tumor cell lines from pleural effusions. J Natl Cancer Inst. 1974; 53:661–674. [PubMed: 4412247]
32. Chambers AF. MDA-MB-435 and M14 cell lines: identical but not M14 melanoma? Cancer Res. 2009; 69:5292–5293. [PubMed: 19549886]
33. Charafe-Jauffret E, Ginestier C, Iovino F, Wicinski J, Cervera N, Finetti P, Hur MH, Diebel ME, Monville F, Dutcher J, et al. Breast cancer cell lines contain functional cancer stem cells with metastatic capacity and a distinct molecular signature. Cancer Res. 2009; 69:1302–1313. [PubMed: 19190339]
34. Ginestier C, Hur MH, Charafe-Jauffret E, Monville F, Dutcher J, Brown M, Jacquemier J, Viens P, Kleer CG, Liu S, et al. ALDH1 is a marker of normal and malignant human mammary stem cells and a predictor of poor clinical outcome. Cell Stem Cell. 2007; 1:555–567. [PubMed: 18371393]
35. Marcato P, Dean CA, Giacomantonio CA, Lee PW. Aldehyde dehydrogenase: its role as a cancer stem cell marker comes down to the specific isoform. Cell Cycle. 2011; 10:1378–1384. [PubMed: 21552008]
36. Ganji PN, Park W, Wen J, Mahaseth H, Landry J, Farris AB, Willingham F, Sullivan PS, Proia DA, El-Hariry I, et al. Antiangiogenic effects of ganetespib in colorectal cancer mediated through inhibition of HIF-1α and STAT-3. Angiogenesis. 2013; 16:903–917. [PubMed: 23838996]
37. Bhola NE, Balko JM, Dugger TC, Kuba MG, Sanchez V, Sanders M, Stanford J, Cook RS, Arteaga CL. TGF-γ inhibition enhances chemotherapy action against triple-negative breast cancer. J Clin Invest. 2013; 123:1348–1358. [PubMed: 23391723]
38. The Cancer Genome Atlas Network. Comprehensive molecular portraits of human breast tumors. Nature. 2012; 490:61–70. [PubMed: 23000897]
39. Semenza GL. Defining the role of hypoxia-inducible factor 1 in cancer biology and therapeutics. Oncogene. 2010; 29:625–634. [PubMed: 19946328]

Key Messages

- Triple-negative breast cancers (TNBCs) respond poorly to available chemotherapy.
- TNBCs overexpress genes regulated by hypoxia-inducible factors (HIFs).
- Ganetespib induces degradation of HSP90 client proteins, including HIF-1α.
- Ganetespib inhibited TNBC orthotopic tumor growth, invasion, and metastasis.
- Ganetespib inhibited expression of HIF-1 target genes involved in TNBC progression.

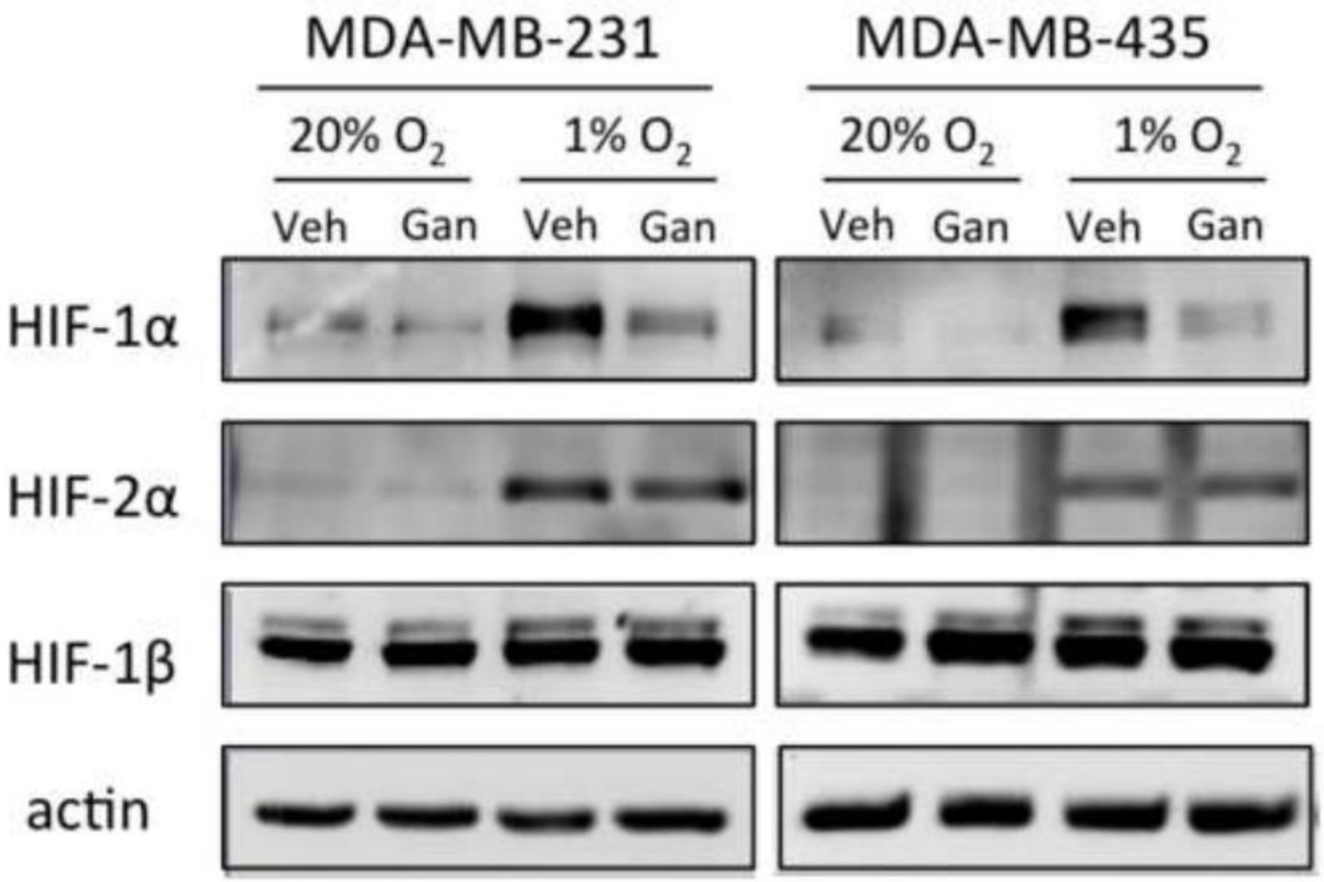

Fig. 1.

Ganetespib treatment inhibits accumulation of HIF-1α in MDA-MB-231 and MDA-MB-435 cells exposed to hypoxia. Cells were pretreated with ganetespib (100 nM) or vehicle for 30 min and exposed to 20% or 1% O2 for 6 h. Whole cell lysates were prepared and aliquots were subjected to immunoblot assay using antibodies against HIF-1α, HIF-2α, HIF-1β, or actin.

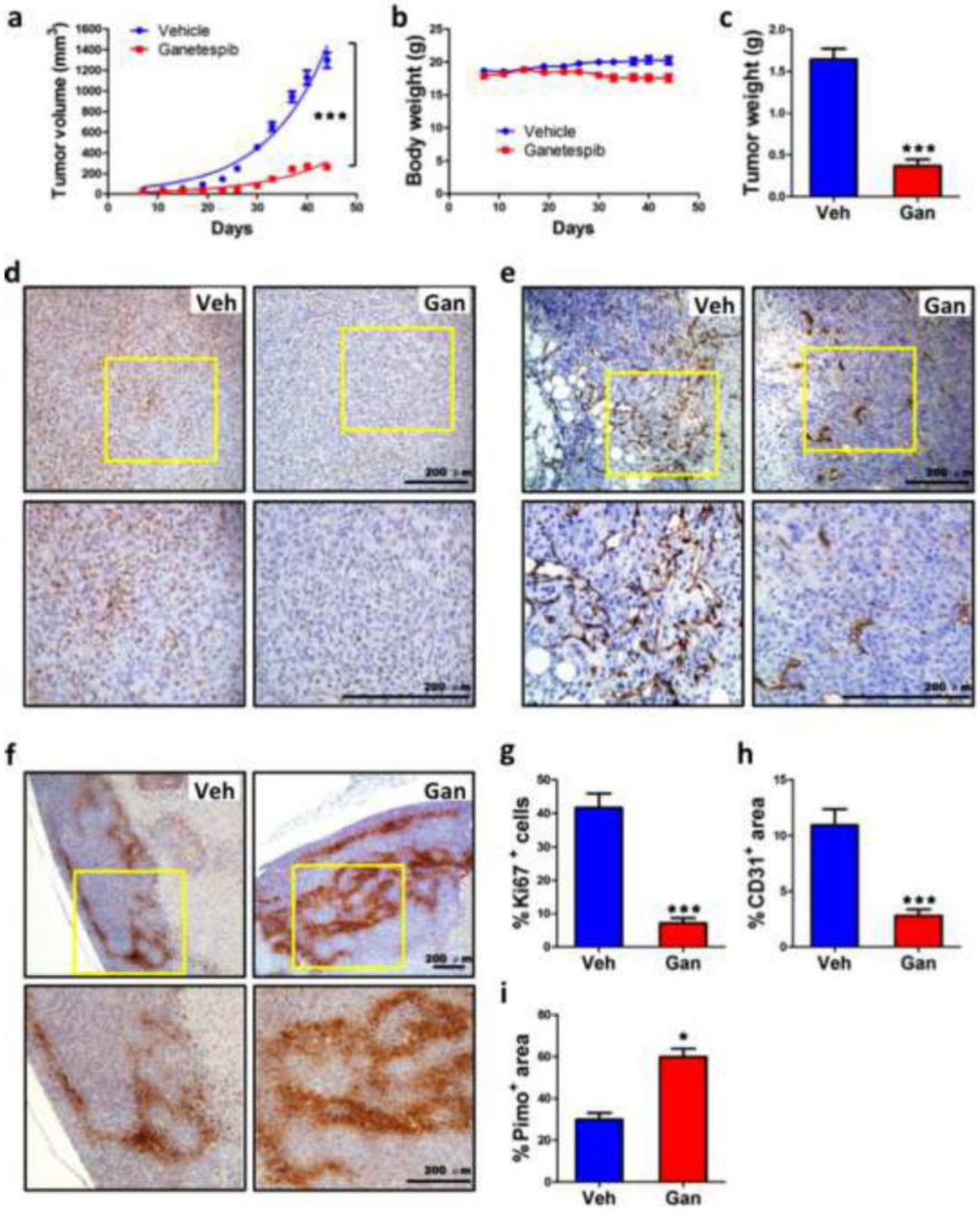

Fig. 2.

Ganetespib treatment inhibits breast tumor growth and vascularization. Severe combined immunodeficiency (SCID) mice received a mammary fat pad injection of 2×10^6 MDA-MB-231 cells. When tumors became palpable, the mice were treated by tail vein injection of vehicle (Veh) or ganetespib (Gan; 150 mg/kg/week) starting on day 7 after orthotopic injection and weekly thereafter. **a-c** Tumor volume (**a**) and body weight (**b**) were determined twice weekly. On day 44, the mice were administered pimonidazole and, 1 h later, tumors were harvested and weighed (**c**). ***$p < 0.001$ vs vehicle, two-way ANOVA or Student's t test (mean ± SEM; $n = 9$). **d-f** Immunohistochemistry was performed on tumor tissue

sections from mice treated with Veh or Gan to analyze cell proliferation by Ki67 staining (**d**), angiogenesis by CD31 staining (**e**), and intratumoral hypoxia by pimonidazole staining (**f**). Representative photomicrographs are shown, with the bottom panel showing higher magnification of the *insert* from the top panel; *scale bar* = 200 μm. ***g-i*** The stained sections were subjected to image analysis and quantification (mean ± SEM); *$p < 0.05$, ***$p < 0.001$ vs vehicle, Student's *t* test.

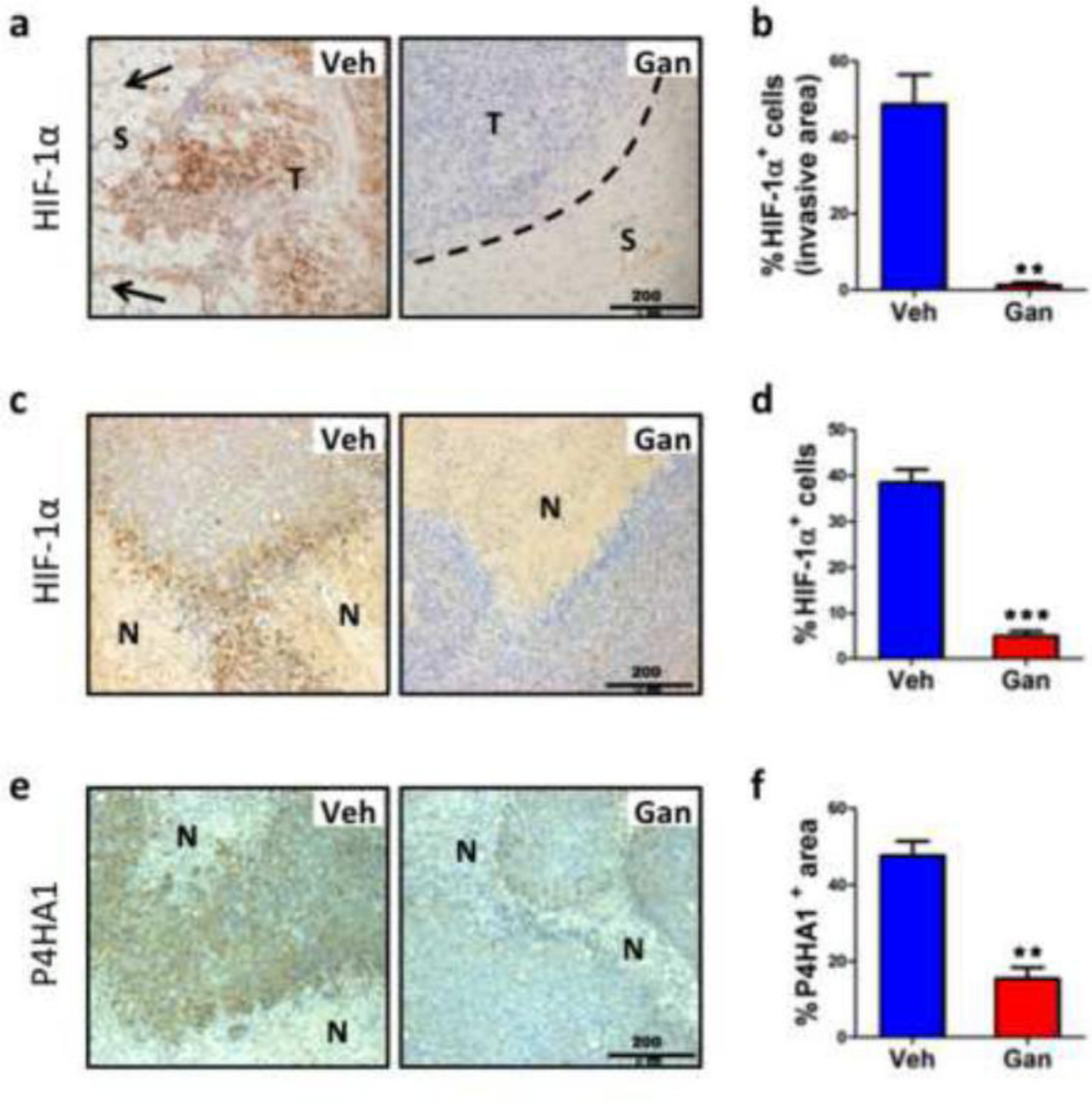

Fig. 3.

Ganetespib treatment inhibits local tissue invasion. **a** Sections from the invasive front of primary tumors from mice treated with Veh or Gan were analyzed by immunohistochemistry for HIF-1α expression. *Arrows* indicate the direction of invasion in Veh section and *dotted line* indicates the well-defined border between tumor (*T*) and stromal tissue (*S*) in Gan section. ***b*** The percentage of cells that were stained for HIF-1α is shown; $^{**}p < 0.01$ vs vehicle, Student's t test (mean ± SEM). **c-f** Adjacent sections from the tumor interior containing areas of necrosis (N) were analyzed by immunohistochemistry for expression of HIF-1α (**c**) or P4HA1 (**e**). *Right:* The percentage of cells in the section that

were stained for HIF-1α (**d**) or P4HA1 (**f**) is shown; $^{**}p < 0.01$, $^{***}p < 0.001$ vs vehicle, Student's t test (mean ± SEM).

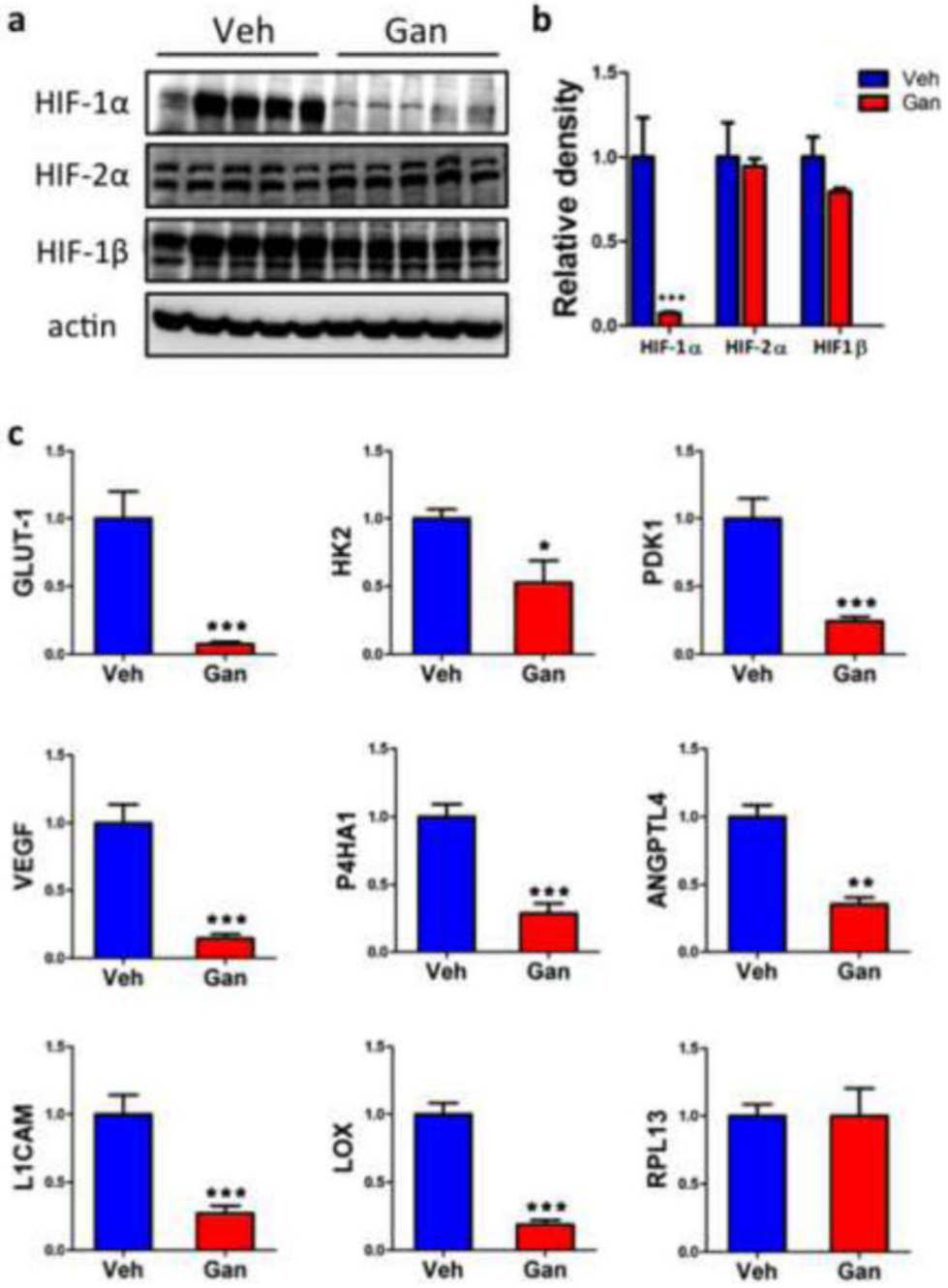

Fig. 4.

Ganetespib treatment inhibits HIF-1α and HIF-1 target gene expression. **a** Tumors from mice treated with vehicle or ganetespib (*n* = 5 each) were lysed and subjected to immunoblot assays with antibodies for HIF-1α, HIF-2α, HIF-1β, or actin. **b** Densitometry was performed and, for each sample, the density ratio of each protein to actin was determined. **c** Total RNA was isolated from tumors harvested from mice treated with vehicle (Veh) or ganetespib (Gan). Reverse transcription (RT) and quantitative real-time PCR (qPCR) were performed using primers specific for mRNA products of established HIF-1 target genes (VEGF, ANGPTL4, GLUT1, HK2, PDK1, L1CAM, LOX, and P4HA1) or a control gene that is not

regulated by HIF-1 (RPL13A). mRNA levels were normalized to 18*S* rRNA levels in the same sample. For all bar graphs, *$p < 0.05$, **$p < 0.01$, ***$p < 0.001$ vs vehicle, Student's t test (mean ± SEM).

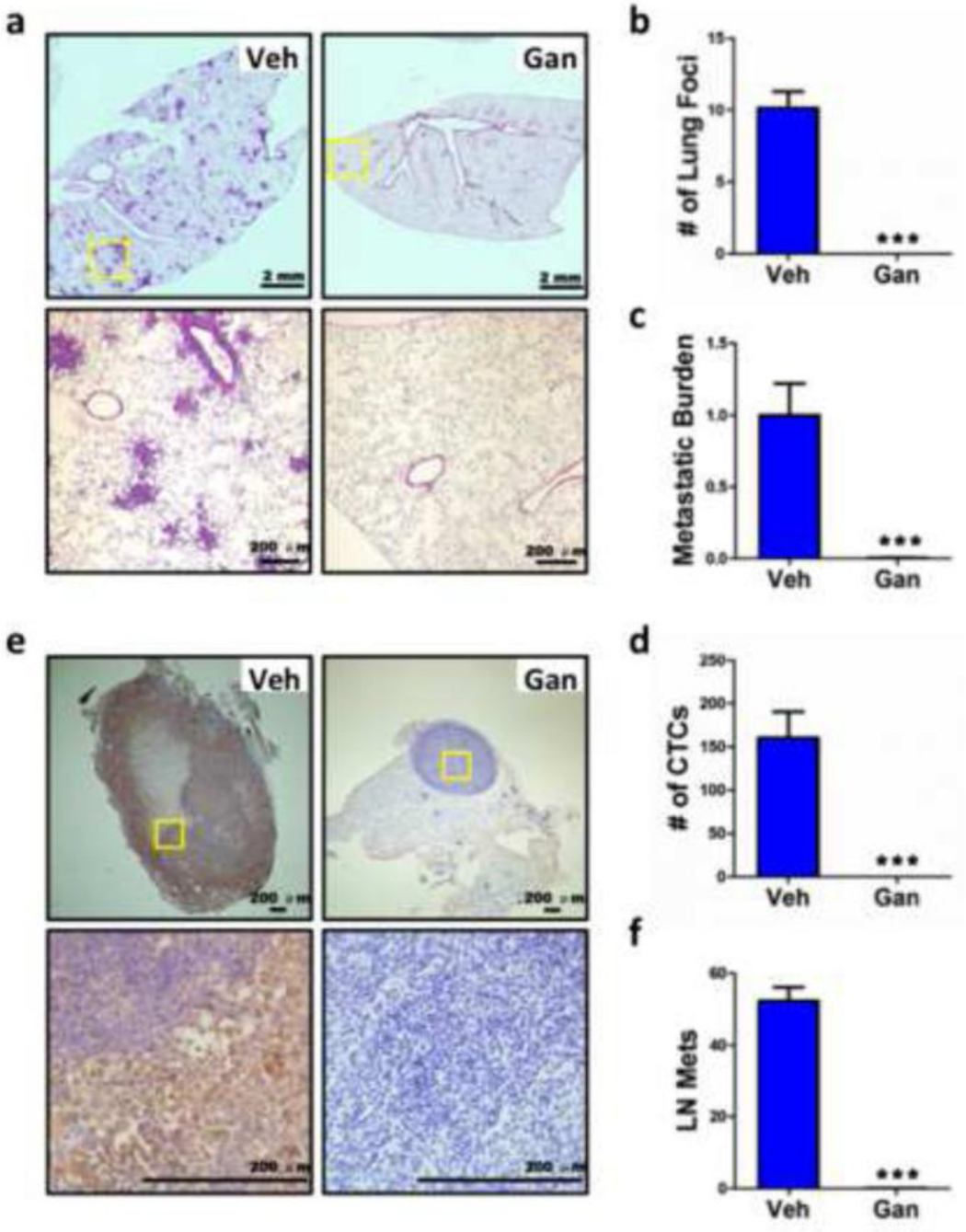

Fig. 5.

Ganetespib treatment inhibits vascular and lymphatic metastasis. Lungs, ipsilateral axillary lymph node, and peripheral blood were also collected on day 44 from tumor-bearing mice treated with vehicle (Veh) and ganetespib (Gan). **a** The left lung was fixed under inflation and sections were stained with hematoxylin and eosin (H&E) to identify metastatic foci. **b** The number of metastatic foci per field (6 random fields per section) was determined. **c** DNA was extracted from the right lung and analyzed by qPCR using primers specific for human *HK2* gene sequences to quantify the total lung metastatic burden. **d** Total cellular RNA isolated from 0.5 ml of peripheral blood was analyzed by RT-qPCR using primers

specific for human 18*S* rRNA as a measure of circulating tumor cells (CTCs). **e** The axillary lymph node ipsilateral to the mammary fat pad injection was harvested and analyzed by immunohistochemistry using an antibody specific for human vimentin. The *lower panel* is a high-power magnification of insert in *upper panel*; *scale bar* = 200 μm. **f** Image analysis was performed to determine the vimentin positive area per field under ×40 magnification based on 6 random fields per section. For all bar graphs, ***$p < 0.001$ vs vehicle, Student's t test (mean ± SEM).

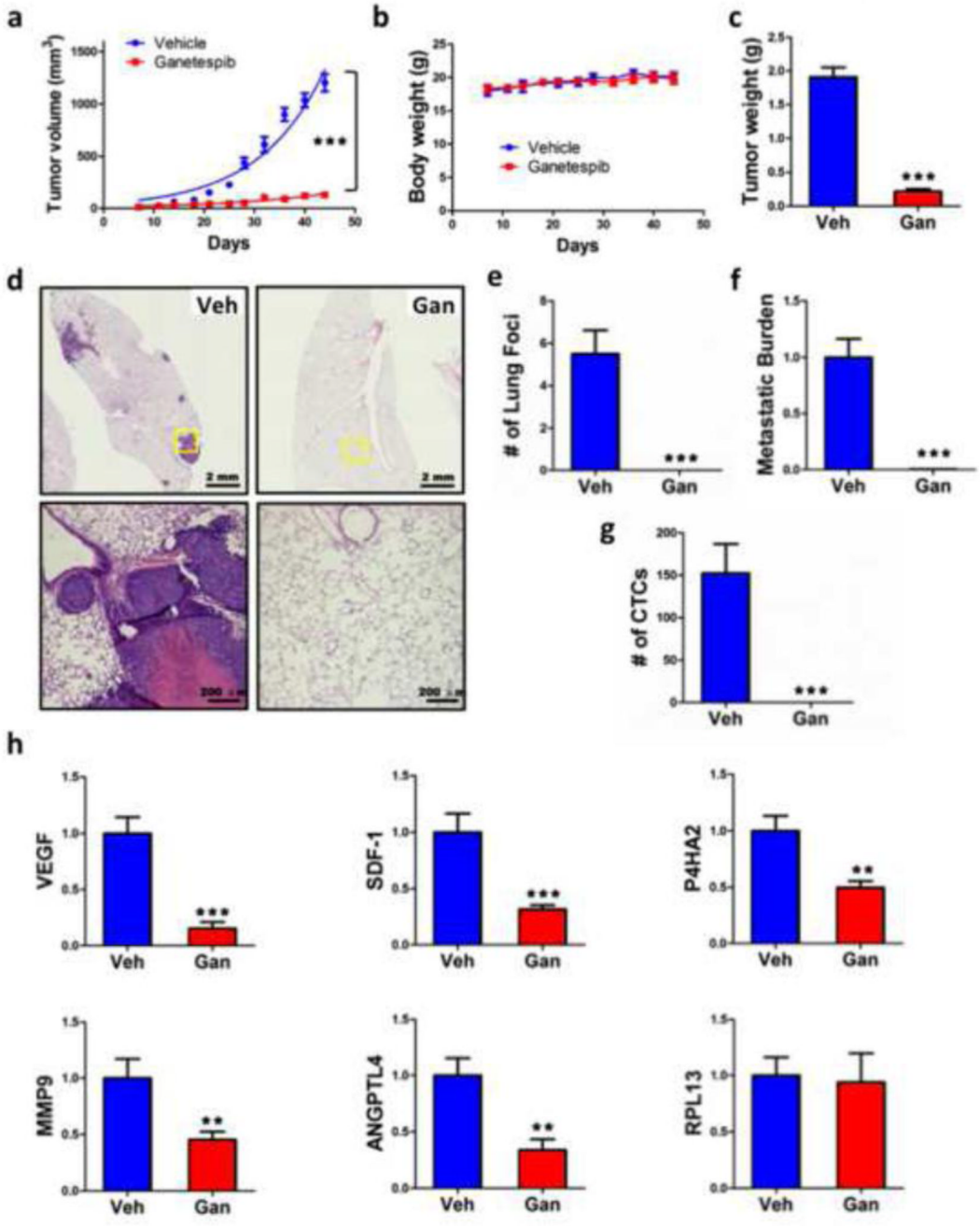

Fig. 6.

Ganetespib treatment inhibits tumor growth, metastasis, and HIF-1 target gene expression following orthotopic transplantation of MDA-MB-435 cells. SCID mice received a mammary fat pad injection of MDA-MB-435 cells followed by tail vein injection of vehicle (Veh) or ganetespib (Gan; 150 mg/kg/week) starting on day 7 after orthotopic injection and weekly thereafter. Tumor volume (**a**) and body weight (**b**) were determined twice weekly and final tumor weight was measured (**c**). Lung sections were stained with H&E (**d**) and the number of metastatic foci per lung section was determined (**e**). Metastatic burden was determined by qPCR of lung genomic DNA using primers specific for the human *HK2* gene

(**f**). CTCs in peripheral blood were determined by RT-qPCR assay of total cellular RNA using primers specific for human 18*S* rRNA (**g**). Total RNA isolated from primary tumors was analyzed by RT-qPCR using primers specific for human VEGF, ANGPTL4, SDF-1, P4HA2, MMP9, and RPL13A mRNA normalized to the levels of 18S rRNA. For all bar graphs, ** $p < 0.01$, *** $p < 0.001$ vs vehicle, two-way ANOVA or Student's t test (mean ± SEM; n = 6).

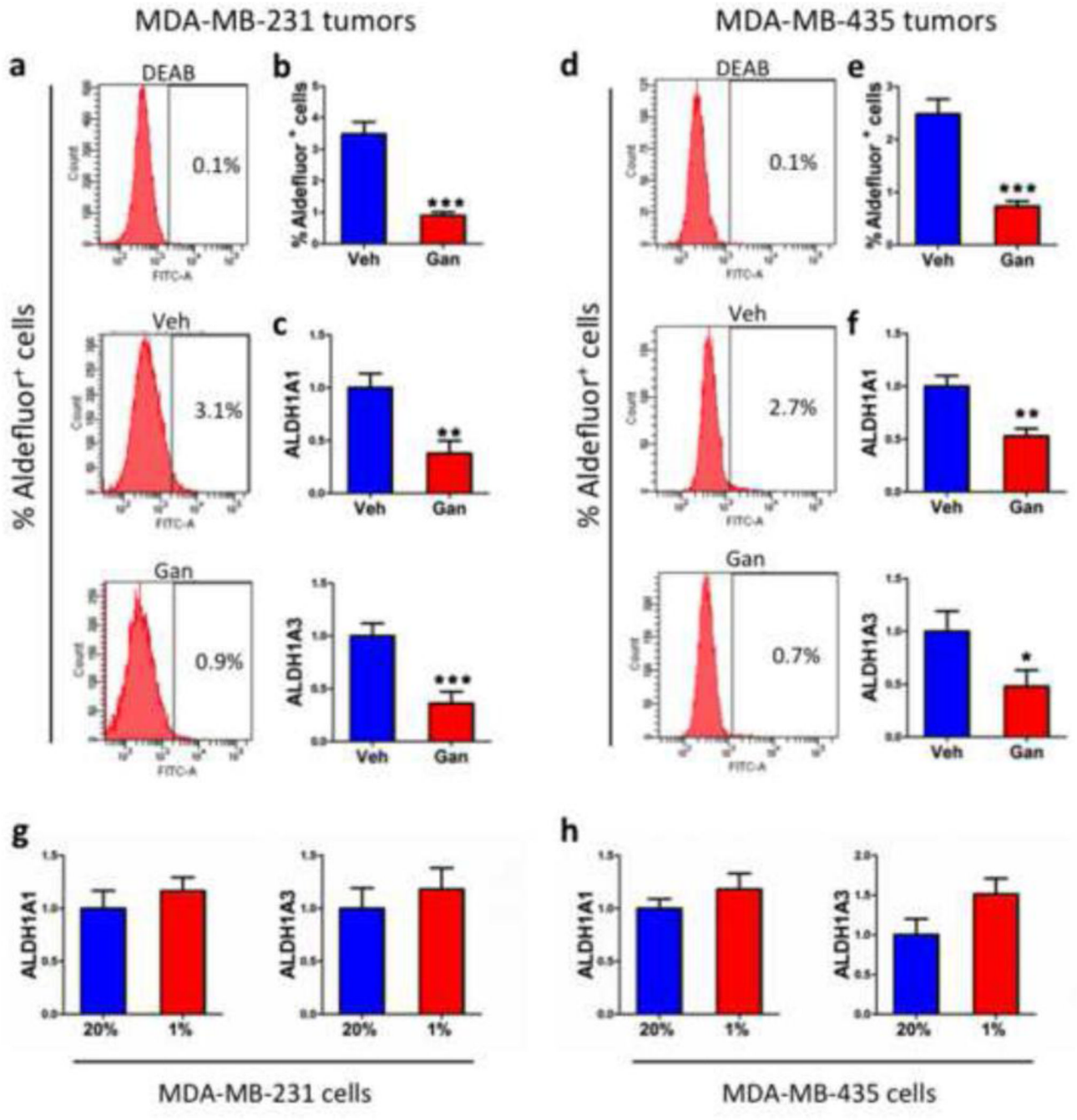

Fig. 7.

Ganetespib treatment reduces the Aldefluor$^+$ cancer stem cell population in primary breast tumors. **a-f** Tumors were harvested on day 44 from mice that received a mammary fat pad injection of MDA-MB-231 (**a-c**) or MDA-MB-435 cells (**d-f**) and were treated with vehicle (Veh) or ganetespib (Gan). Single cell suspensions were prepared from the tumors, incubated with a fluorogenic substrate of aldehyde dehydrogenase, and the percentage of cells that were Aldefluor$^+$ was determined by flow cytometry. Representative histograms are shown for tumor cells incubated with the aldehyde dehydrogenase inhibitor DEAB as a negative control (*top panel in **a** and **d***); tumor cells from a vehicle-treated mouse (*middle*

*panel in **a** and **d***); and tumor cells from a ganetespib-treated mouse (*bottom panel in **a** and **d***). The percentage of Aldefluor$^+$ cells (**b** and **e**) and the ALDH1A1 and ALDH1A3 mRNA levels (**c** and **f**) in primary tumors were determined. **g-h** MDA-MB-231 (**g**) and MDA-MB-435 (**h**) cells were cultured in the presence or 20% or 1% O2 for 24 h and ALDH1A1 and ALDH1A3 mRNA levels were quantified by RT-qPCR. For all bar graphs, *$p < 0.05$, **$p < 0.01$, ***$p < 0.001$ vs vehicle, Student's t test (mean ± SEM).

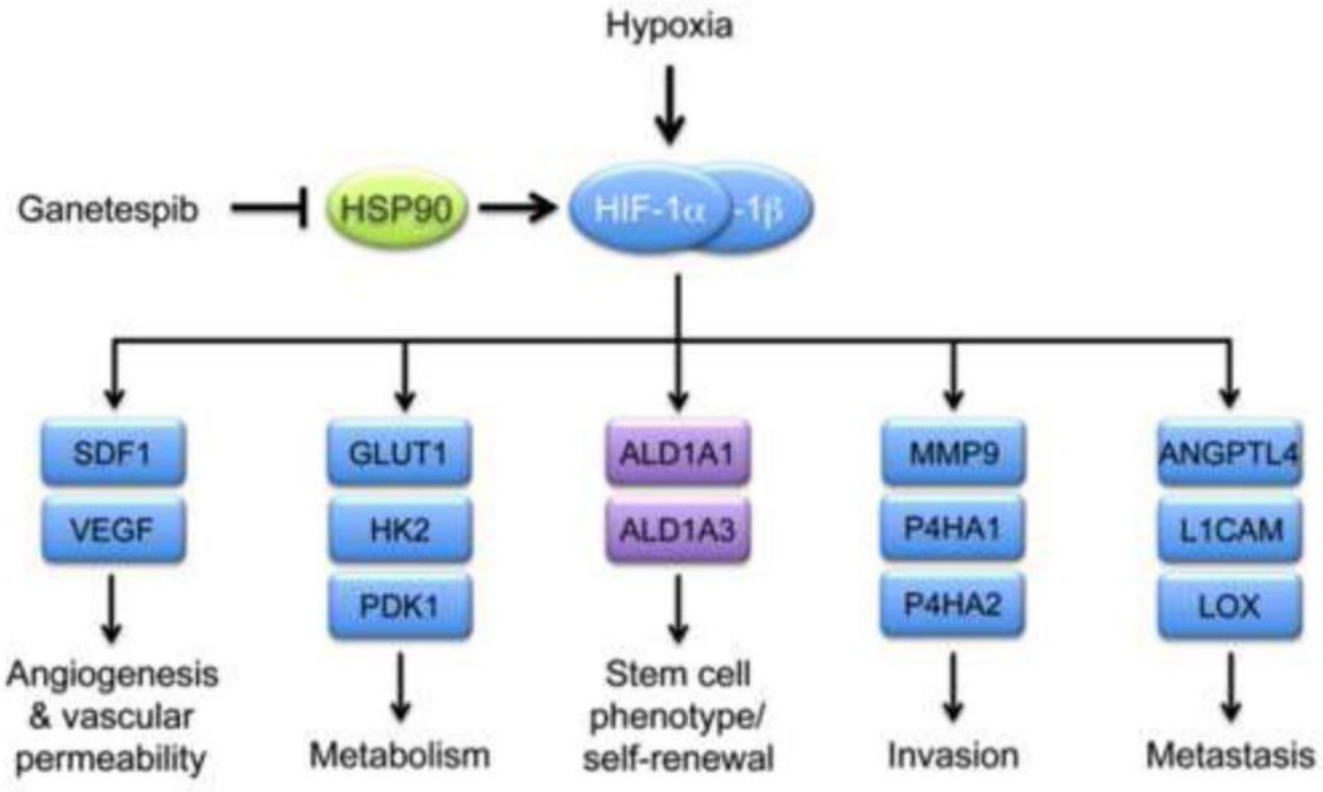

Fig. 8.

Consequences of HIF-1α inhibition by ganetespib in triple-negative breast cancer cells. Ganetespib inhibits HSP90-dependent stabilization of HIF-1α and transcription of HIF-1 target genes (*blue rectangles*) whose protein products mediate angiogenesis and vascular permeability (SDF1, VEGF), glycolytic metabolism (GLUT1, HK2, PDK1), invasion (MMP9, P4HA1, P4HA2), and metastasis (ANGPTL4, L1CAM, LOX). Ganetespib also reduced the number of Aldefluor^{+} cancer stem cells and decreased ALDH1A1 and ALDH1A3 mRNA levels, although the latter genes (*purple rectangles*) are not directly regulated by HIF-1 in breast cancer cells.